Characterization of Carbon Concentrates from Coal-Combustion Fly Ash

John P. Baltrus,* Arthur W. Wells, Daniel J. Fauth, J. Rodney Diehl, and Curt M. White

U.S. Department of Energy, National Energy Technology Laboratory, P.O. Box 10940, Pittsburgh, Pennsylvania 15236-0940

A study of carbon concentrates separated by a number of different commercial and laboratory methods from various coal-combustion fly ashes was undertaken to determine what common and unique chemical and physical properties can be expected in such concentrates. The properties were determined using a variety of physical and spectroscopic characterization methods and then were compared among the carbon concentrates and in two cases with the properties of the unprocessed fly ashes. The class F fly ashes originated from a total of seven different utilities burning bituminous coals and underwent one of six different processing methods to produce the carbon concentrates, which contained from 24% to 76% carbon. Three different configurations of triboelectrostatic separators were used to produce the carbon concentrates in addition to two different flotation methods plus a proprietary carbon recovery process. The results showed that unburned carbon concentrates from fly ash have properties similar to most carbon blacks and would be poor replacements for activated carbon in adsorption processes unless they are activated in a separate step. The untreated carbon may have applications as a substitute for carbon black provided it could be obtained in sufficient purity. The results have implications for those who wish to use carbon concentrates from coal-combustion fly ashes in secondary markets, especially as sorbents and fillers.

Introduction

An increase in carbon content of coal-fired utility fly ashes has been a significant concern since the introduction of low-NO_x burners to control the emission of nitrogen oxides during coal combustion.[1] A loss-on-ignition (LOI) value greater than 6% (ASTM C618-00) for fly ash prohibits its primary use as a supplemental material in cement and concrete. Utility fly ashes containing significant quantities of carbon must undergo processing to reduce their carbon content before they can be added to cement and concrete; otherwise they are generally disposed of in a landfill.[2] Both of these scenarios add to electric generation costs.

A number of different processes have been developed for separating carbon from utility fly ash.[3,4] They can be classified into the two general categories of either dry or wet separation. Dry separation usually involves sieving or triboelectrostatic technologies,[5] or a combination of both. Wet separation can be accomplished using froth flotation[6,7] or agglomeration.[8,9]

Some of the ash processing costs can be recovered by selling the carbon-depleted product ash as a pozzolanic material. There is a limited market for the carbon-enriched product of fly ash separation processes and in many cases that portion is still disposed of in a landfill. The carbon-enriched portion of fly ash could be reburned, but recent studies have demonstrated other possible uses for it. The carbon can be used as a catalyst.[10] It can also be activated and then substituted in applications that typically use activated carbons.[9,11,12] Those applications include mercury adsorption[13,14] and

* Author to whom correspondence should be addressed. Fax: 412-386-4806. E-mail: baltrus@netl.doe.gov.

(1) Hower, J. C.; Rathbone, R. F.; Robl, T. L.; Thomas, G. A.; Haeberlin, B. O.; Trimble, A. S. *Waste Manage.* **1997**, *17*, 219−229.

(2) Larrimore, L. *Proceedings of the 2000 Conference on Unburned Carbon on Utility Fly Ash*; U.S. DOE National Energy Technology Laboratory: Pittsburgh, 2000; p 5.

(3) Coates, M. E. *Proceedings of the 2000 Conference on Unburned Carbon on Utility Fly Ash*; U.S. DOE National Energy Technology Laboratory: Pittsburgh, 2000; pp 39−42.

(4) Soong, Y.; Baltrus, J.; Champagne, K. J.; Fauth, D. J.; Gray, M. L.; Knoer, J. P.; Link, T. A.; Newby, T. L.; Sands, W. D.; Schoffstall, M. R. *Proceedings of the 1999 Conference on Unburned Carbon on Utility Fly Ash*; U.S. DOE Federal Energy Technology Center: Pittsburgh, 1999; pp 23−25.

(5) Ban, H.; Li, T. X.; Hower, J. C.; Schaefer, J. L.; Stencel, J. M. *Fuel* **1997**, *76*, 801−805.

(6) Hwang, J. Y. U.S. Patent 5,047,145, 1991.

(7) Groppo, J. G.; Brooks, S. M. U.S. Patent 5,456,363, 1995.

(8) Gray, M. L.; Champagne, K. J.; Soong, Y. *Proceedings of the 2000 Conference on Unburned Carbon on Utility Fly Ash*; U.S. DOE National Energy Technology Laboratory: Pittsburgh, 2000; p 75.

(9) DeBarr, J. A.; Rapp, D. M.; Rostam-Abadi, M.; Rood, M. J. *Prepr. Pap.—Am. Chem. Soc., Div. Fuel Chem.* **1996**, *41*, 604−608.

(10) Finseth, D. H.; Kaufman, P. B.; Mathur, M.; Harris, M.; Farcasiu, M. *DGMK Tagungsber.* **1997**, 9704 (Proceedings ICCS'97, Vol. 3), pp 1919−1922.

(11) Maroto-Valer, M. M.; Taulbee, D. N.; Schobert, H. H. *Prepr. Pap.—Am. Chem. Soc., Div. Fuel Chem.* **1999**, *44*, 101−105.

(12) Maroto-Valer, M. M.; Andresen, J. M. *Proceedings of the 2000 Conference on Unburned Carbon on Utility Fly Ash*; U.S. DOE National Energy Technology Laboratory: Pittsburgh, 2000; pp 21−23.

(13) Hower, J. C.; Maroto-Valer, M. M.; Taulbee, D. N.; Sakulpitakphon, T. *Energy Fuels* **2000**, *14*, 224−226.

(14) Granite, E. J.; Pennline, H. W.; Hargis, R. A. *Ind. Eng. Chem. Res.* **2000**, *39*, 1020−1029.

Table 1. Sample Properties

sample	origin	concentration process	% C
UK1A	University of Kentucky Center for Applied Energy Research (CAER)	Parent Dale Power Station Fly Ash	30.0
UK1B		Dale Power Station Fly Ash Single run − cylindrical dry separator	52.2
UK1C		Dale Power Station Fly Ash Single run − parallel plate triboelectrostatic separator	67.1
UK1D		Dale Power Station Fly Ash Double run − parallel plate triboelectrostatic separator	73.0
UK2		Unnamed pond fly ash sample processed using the Fast Float Process[a]	63.7
PMET1	Pittsburgh Mineral & Environmental Technology, Inc.	Ohio utility fly ash − sized followed by wet separation	75.9
PMET2		Canadian utility fly ash − sized followed by wet separation	57.3
NEP1	New England Power	Unprocessed fly ash from Salem Harbor Power Station	19.8
NEP2		Brayton Point Power Station fly ash processed using Separations Technology Inc. (STI) triboelectrostatic system	24.3
MTU1	Michigan Tech University	Froth flotation[b] of Baltimore Gas & Electric fly ash	38.6
MTU2		Froth flotation[b] of American Electric Power Co. fly ash	73.3

[a] See ref 7. [b] See ref 6.

adsorption of organic[15,16] and organo-metallic compounds.[17] Unburned carbon can also be used in carbon artifacts or as a filler material.[12,18]

The best applications for the unburned carbon separated from coal-combustion fly ash will be those that can utilize carbon from a wide range of fly ash sources. Therefore, it is important to determine what general chemical and physical properties can be expected of carbons separated from a variety of fly ashes using a number of separation processes. It has already been shown that the properties of fly ashes can vary significantly based upon their origin.[19,20]

A general understanding of the properties of unburned carbon can be somewhat assembled from several studies focusing on its specific properties and behavior.[21−25] Those studies have usually focused on characterization of the properties of a limited number of ash-derived carbons, or only a few characterization methods have been employed in a given study. The present study was undertaken to determine the variability, or lack thereof, of some of the most important properties of carbons across a broad spectrum of carbon concentrates from different coal-combustion fly ashes and produced by a number of commercial and laboratory separation methods. The results have implications for those who wish to use carbon concentrates from coal-combustion fly ashes in secondary markets, especially as sorbents and fillers.

Samples and Experimental Techniques

A series of nine carbon concentrates derived from coal-combustion fly ashes and having carbon concentrations ranging from 24% to 76% plus two unprocessed ashes, also having high concentrations of carbon, were examined using a variety of physical and spectroscopic methods. Information about the origin of the samples used in this study is summarized in Table 1. The samples originated from a total of seven different coal-fired utilities, all burning bituminous coals using low-NO_x burners. Six different methods were used to produce the carbon concentrates. The samples were grouped primarily on the basis of their origin as determined by the facilities and methods used to process the ash. Less was known about the utilities where the unprocessed ashes were collected, other than what information was provided by the processors of the ashes. Carbon concentrations were determined using ASTM Method D3178-89.

Physical Property Measurements. The multi-point specific surface area was determined using nitrogen adsorption at 77 K over the relative pressure range $P/P_0 = 0.03$ to 0.3. Bulk density, which includes the pore volume of the particles and the interparticle space, was measured using ASTM Method D2854-96. Envelope density, which includes the volume occupied by the sample's skeleton and pores, was measured using mercury porosimetry (ASTM Method C493−93). Skeletal density, which excludes the volume of the sample pores, was measured using helium pycnometry. Macropore (>50 nm diameter) and mesopore (2−50 nm diameter) volume distributions and average pore diameters were also calculated from the mercury porosimetry measurements. Micropore (<2 nm diameter) volumes were not measured directly. Rather they were determined by difference from the results of mercury porosimetry and helium pycnometry.[26] Particle size measurements were performed using an Elzone 5380 particle analyzer.

Because the carbon concentrates are being considered for applications that typically employ activated carbon, some of the adsorption measurements commonly used to evaluate activated carbons were carried out on the carbon concentrates. One such measurement, iodine number, usually correlates with the surface area of the carbon and was determined for each sample using ASTM Method D4607-94. Carbon tetrachloride activities are used to approximate pore volumes in activated carbons and were measured using ASTM Method D3467-99.

Thermal Analyses. Thermogravametric analyses (TGA) were carried out in air over a temperature range of ambient to 1000 °C at a heating rate of 10 °C/min. Approximately 10 mg of sample was used for each TGA experiment. Controlled-

(15) Jain, K. K.; Prasad, G.; Singh, V. N. *J. Chem. Technol. Biotechnol.* **1979**, *29*, 36−38.
(16) Graham, U. M.; Robl, T. L.; Rathbone, R. F. *Prepr. Pap.—Am. Chem. Soc., Div. Fuel Chem.* **1996**, *41*, 265−269.
(17) Graham, U. M.; Groppo, J. G.; Robl, T. L. *Prepr. Pap.—Am. Chem. Soc., Div. Fuel Chem.* **1998**, *43*, 985−989.
(18) Andresen, J. M.; Maroto-Valer, M. M.; Andresen, C. A.; Battista, J. J. *Proceedings of the 1999 International Ash Utilization Symposium*; Lexington, 1999; pp 534−540.
(19) Quann, R. J.; Neville, M.; Sarofim, A. F. *Combust.n Sci. Technol.* **1990**, *74*, 245−265.
(20) Boni, C.; Cereda, E., Marcazzan, G. M. B.; Parmigiani, F. *Combust. Effic. Air Qual.* **1995**, 213−240.
(21) Hill, R. L.; Sarkar, S. L.; Rathbone, R. F.; Hower, J. C. *Cem. Concr. Res.* **1997**, *27*, 193−204.
(22) Hill, R. L.; Rathbone, R. F.; Hower, J. C. *Cem. Concr. Res.* **1998**, *28*, 1479−1488.
(23) Smith, K. A.; Kulaots, I.; Hunt, R. H.; Suuberg, E. M. *Proceedings of the 1997 International Ash Utilization Symposium*; Lexington, 1997; pp 650−657.
(24) Hower, J. C.; Thomas, G. A.; Clifford, D. J.; Eady, J. D.; Robertson, J. D.; Wong, A. S. *Energy Sources* **1996**, *18*, 107−118.
(25) Hurt, R. H.; Davis, K. A.; Yang, N. Y. C.; Headley, T. J.; Mitchell, G. D. *Fuel* **1995**, *74*, 1297−1306.
(26) Shields, J. E.; Lowell, S. *Powder Technol.* **1983**, *36*, 1−4.

Table 2. Physical Properties of Carbon Concentrates

	carbon %	surface area (m^2/g)	bulk density (g/cm^3)	envelope density (g/cm^3)	skeletal density (g/cm^3)	pore volumes (mL/g)			average pore diameter (μm)	reflectance %
						macro	meso	micro[a]		
UK1A	30.0	17.8	0.259	0.752	2.42	0.846	0.161	−0.090	0.046	7.81
UK1B	52.2	27.4	0.259	0.639	2.39	1.017	0.144	−0.014	0.064	7.86
UK1C	67.1	36.0	0.270	0.570	2.49	1.207	0.180	−0.034	0.057	7.82
UK1D	73.0	36.8	0.264	0.559	3.08	1.151	0.156	0.158	0.064	7.71
UK2	63.7	25.8	0.265	0.371	2.13	1.770	0.216	0.243	0.072	7.28
PMET1	75.9	16.7	0.279	0.279	1.93	2.756	0.154	0.156	0.143	7.58
PMET2	57.3	24.0	0.270	0.260	2.16	3.312	0.213	−0.142	0.127	7.51
NEP1	19.8	13.6	0.269	0.544	2.20	1.030	0.208	0.147	0.044	7.77
NEP2	24.3	12.0	0.261	0.867	2.30	0.753	0.196	−0.230	0.037	7.99
MTU1	38.6	28.7	0.265	0.553	2.68	1.241	0.208	−0.014	0.052	7.94
MTU2	73.3	33.2	0.257	0.331	2.36	2.187	0.220	0.188	0.085	8.42

[a] Determined by difference (1/envelope density − 1/ skeletal density − macropore volume − mesopore volume).

atmosphere programmed-temperature oxidation (CAPTO) profiles of fly ash were produced as previously described.[27] Individual 50 mg samples of the carbon concentrates were heated at 3 °C/min from ambient temperature to 1050 °C. Plug flow (Reynolds number ≅ 100) of 10% oxygen/90% argon through the samples during thermal treatment ensured uniform reaction throughout the sample plug.

Spectroscopic Measurements. Raman spectra were collected using a Raman microprobe and the 632.8 nm line from a HeNe laser excitation source. The laser was focused onto the sample using a combination of a cylindrical lens and a 50× (0.8 N.A.) infinity-corrected objective. This combination produced a line focus 4 μm wide and 40 μm long. The configuration was employed to improve the sampling statistics of the method. All spectra presented are the result of 10 signal-averaged scans collected at 4 cm^{-1} resolution using an integration time of 30 s per point. Samples were prepared for analysis by pressing them into pellets under moderate pressure. Incident power into the microscope was 2 mW, which was distributed over the area previously mentioned.

X-ray diffraction (XRD) patterns were obtained with a computer-controlled diffractometer equipped with a long fine-focus copper X-ray tube, a diffracted beam graphite monochromator to provide monochromatic Cu Kα radiation, and a scintillation detector. When collecting data from the samples, step-scans were made at 0.1° intervals, and counting times varied from 5 to 60 s per step according to the intensity of the diffraction peak.

A reflected light microscope was used to acquire images of the carbon concentrates. Bright-field illumination was used at various magnifications. A small quantity of carbon powder was placed on a glass slide using a spatula and then the slide was tapped until the powder was well dispersed.

For petrographic analyses, portions of each sample were mounted in epoxy, ground, and polished for microscopic analysis and preparation of photomicrographs using reflected light. Relative mean-maximum reflectance measurements were obtained using a microscope equipped with a polarizer set at 45°. A magnification of about 450× was used and the stage rotated through 360° to obtain maximum reflectance. Because of the particle size, the number of determinations was limited to 25 readings.

Results

Physical Properties. The BET surface areas, densities, pore volume distributions, and average pore diameters of the carbon concentrates are reported in Table 2. There was not much variation in many of the values between different carbon concentrates. Surface areas ranged from 12 m^2/g to 37 m^2/g. The measured bulk densities averaged 0.265 ± 0.006 g/cm^3. There was more variation in envelope density between the samples, while skeletal density ranged from 2 to 3 g/cm^3. The greatest fraction of the pore volume was found in macropores. The mesopore volume was 10% or less of the macropore volume and the micropore volume was equally small or nonexistent. In several cases, a small but negative value is reported for micropore volume in Table 2. The significance of the negative values will be discussed later. The pore volume distribution was essentially unimodal and asymmetric. The average pore diameter, as determined by mercury porosimetry, ranged from 0.4 to 0.8 μm except for the two PMET samples, which had values that were generally twice those for the other carbon concentrates.

The carbon concentrates showed no significant adsorption activity as measured by iodine numbers and carbon tetrachloride activities. Both measurements yielded values that were extremely low; not existing for all practical purposes. Iodine numbers were less than 20 mg/g for all samples and carbon tetrachloride activities were less than 0.20 wt %.

The results of the mercury porosimetry measurements are shown graphically in Figure 1. The plot of the incremental intrusion versus pore diameter shows that most of the pore volume can be attributed to pores between 0.3 and 1 μm in diameter except for the PMET samples, where the pore diameter distribution is shifted to higher values.

The most important results of the particle size analyses are represented by the data reported in Table 3. The instrument yields a distribution of particle counts versus the equivalent spherical diameters of the particles. For all of the samples in this study, a log-normal distribution of particle sizes was found. As is common practice with such distributions, the geometric mean and geometric standard deviations are reported.

The greatest number of particles had equivalent spherical diameters of approximately 1 μm. They typically ranged in size between 0.8 and 5 μm with the exception of the PMET samples and the NEP1 sample, which were, respectively, higher and lower than that range. Also included in the particle size report was a particle volume report. The particle volume distribution was generated by converting the particle diameters to volume using the formula $V = 4/3\ \pi r^3$. Although a majority of the particles were between 0.8 and 5 μm, most of the volume occupied by the sample could be

(27) LaCount, R. B.; Kern, D. G.; Shriver, J. S.; Banfield, T. L. *Proceedings of the 1997 Conference on Unburned Carbon on Utility Fly Ash*; U.S. DOE Federal Energy Technology Center: Pittsburgh, 1997; pp 67−73.

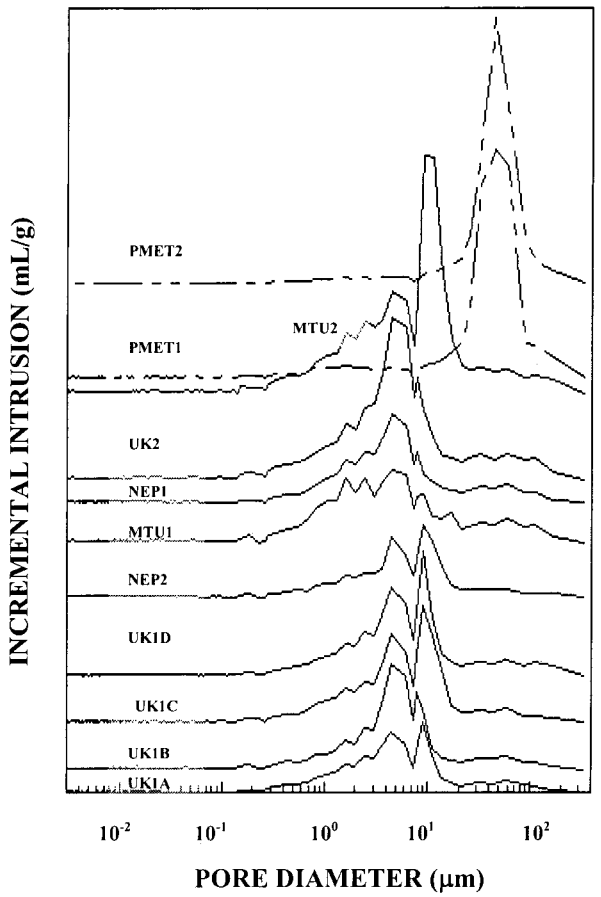

Figure 1. Incremental intrusion of mercury as a function of pore diameter of the carbon concentrates. Curves for the PMET samples are shown with dashed lines.

Table 3. Particle Size Analysis Results

sample	geometric mean size (μm)	geometric standard deviation (μm)
UK1A	1.945	1.728
UK1B	2.621	1.930
UK1C	1.710	1.791
UK1D	1.707	1.807
UK2	1.097	1.628
PMET1	17.91	1.880
PMET2	40.98	1.837
NEP1	0.721	1.923
NEP2	1.440	1.683
MTU1	1.711	1.629
MTU2	1.487	1.643

attributed to the small percentage of particles larger than that range.

Thermal Analyses. The CAPTO profiles of the samples are shown in Figure 2. Similarly the TGA profiles are shown in Figure 3. The TGA profiles have been manipulated so they are more easily compared with the CAPTO profiles by plotting the negative derivative of the weight versus temperature curve as a function of temperature. The curves produced for a given sample by the two methods of thermal analysis were nearly identical in peak shape and position. Except for the PMET sample, the curve shapes were also very similar among the different samples, showing that peak oxidation of carbon occurred between 600 and 650 °C.

Spectroscopic Measurements. Raman spectra of the samples are shown in Figure 4. The spectra feature a very broad band at 1360 cm^{-1} and a somewhat less intense and narrower band at 1630 cm^{-1}.

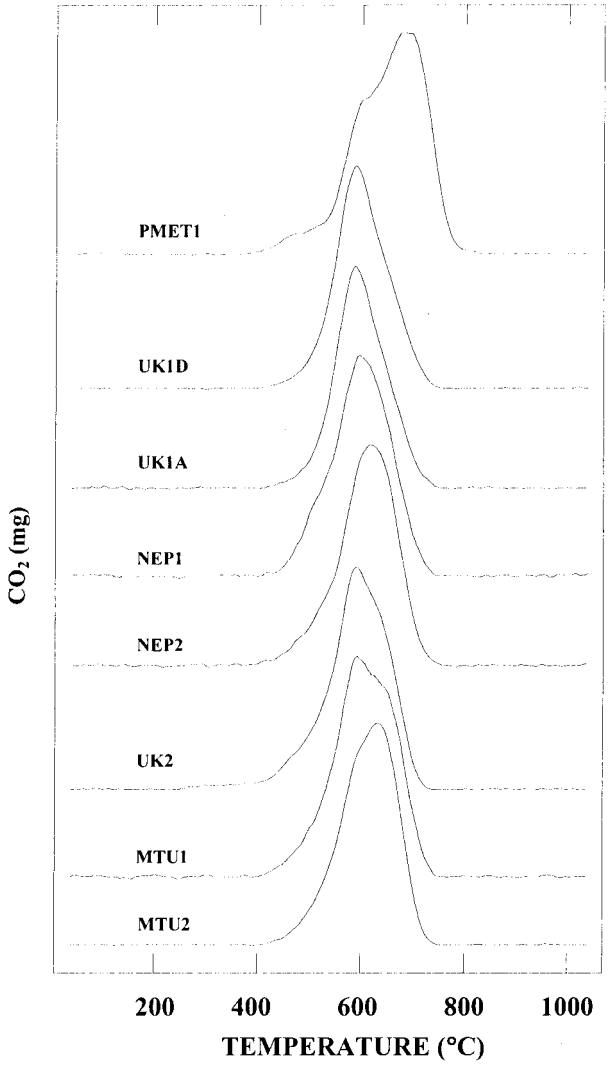

Figure 2. CAPTO carbon dioxide evolution profiles for the carbon concentrates.

Broad features due to amorphous carbon and other noncrystalline structures dominated the X-ray diffraction patterns. Depending on the purity of the carbon concentrates, significant quantities of crystalline quartz and alumino-silicates were detected. Trace amounts of $CaCO_3$, $CaSO_4$, and iron oxides were also found in some samples.

The petrographic analyses showed some general microtexture features that were common to all samples. The principal char type in most of the samples contained thicker walled pores, although the carbons typically were of low or medium porosity. Only the UK2 fly ash exhibited thinner walled pores. Anisotropic features were dominant in all of the carbon concentrates. The UK2 sample was the only one that exhibited a significant amount of isotropic carbon. It should be noted that the structure of many of the carbon particles in the PMET1 sample appeared similar to metallurgical coke. Relative mean−maximum reflectance values are reported in Table 2 and range from 7.28% to 8.42%.

Microscopic image analysis at 20× magnification generally confirmed what was already known from particle size analyses. The char particles had irregular shapes and in many cases the particles remained agglomerated despite efforts to disperse them. Repre-

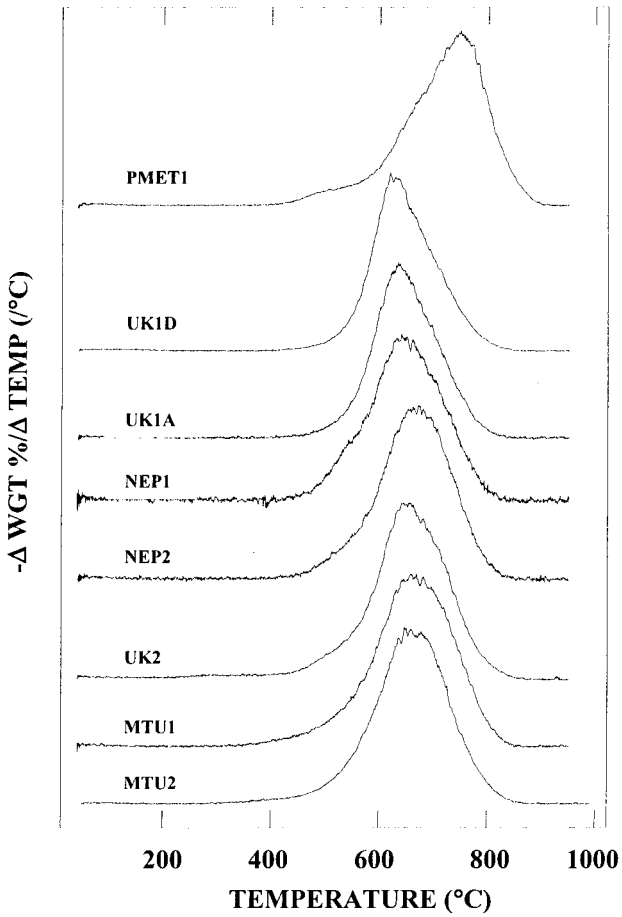

Figure 3. TGA profiles of the carbon concentrates. The derivative of the weight loss vs temperature curve is plotted as a function of temperature.

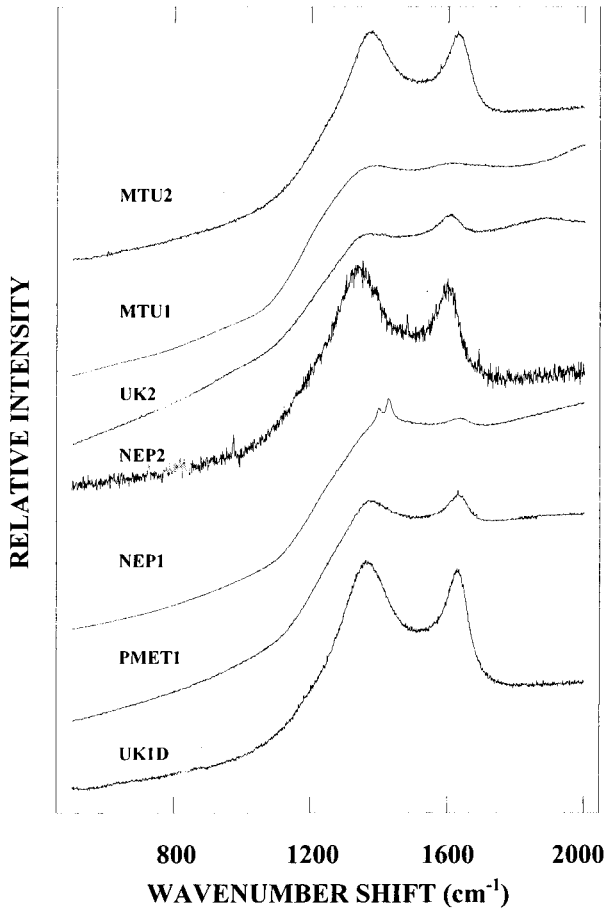

Figure 4. Raman spectra of the carbon concentrates.

sentative images are shown in Figures 5 and 6 for two UK1 samples before and after carbon enrichment, respectively. These images, taken at the same magnification, can help one visualize the effects of the triboelectrostatic enrichment process on carbon and ash in fly ash. The parent fly ash in Figure 5 contains agglomerates of ash and char. There are very small carbon particles (black) trapped within and attached to larger ash particles (grayish white). There are also larger char particles with small ash particles interlocked within the char. The particle sizes are reduced considerably following triboelectrostaic separation (Figure 6).

Discussion

As displayed in Table 1, this study utilized a diverse set of samples. The flyash samples contained between 20% and 76% carbon depending on the process used to concentrate the carbon. Two of the samples, NEP1 and UK1A, were unprocessed high-carbon ashes. The remaining samples were processed either by mechanical or wet separation except for the PMET samples, which were processed first by mechanical means (sieving) and then by wet separation (flotation). The UK1 series of samples allows one to compare the effects of two types of triboelectrostatic separation and repetitive processing on the same starting material. Because of the diverse nature of the samples, excellent insight is obtained into what important chemical and physical properties are common over a wide range of carbon concentrates.

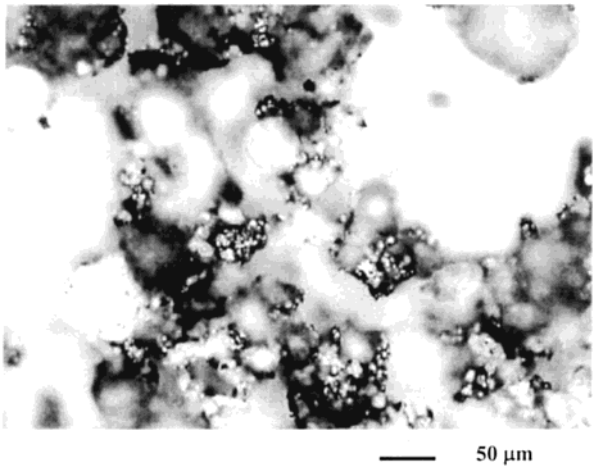

Figure 5. Image of sample UK1A particles (30% C).

None of the samples revealed any activated carbon-like physical properties. One of the most important characteristics of activated carbons is their high surface area, typically on the order of several hundred m^2/g. As reported in Table 2, all of the carbon concentrates have very low surface areas. As noted in previous studies, the mineral matter portion of the concentrates does not contribute significantly to the measured surface areas.[21] Such low surface areas are typical of carbons derived from class F fly ashes, which result from the burning of low-calcium bituminous coals.[28]

Other physical characteristics of the carbons also are not consistent with the properties desired of activated carbons. An average bulk density of 0.264 g/cm^3 meas-

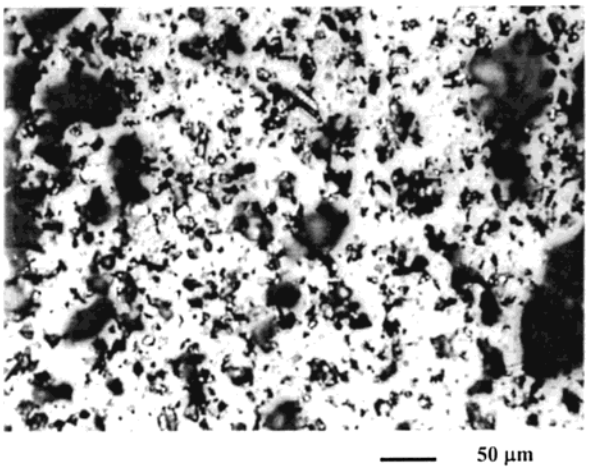

Figure 6. Image of sample UK1D particles (73% C), which were obtained by processing sample UK1A twice through a parallel plate triboelectrostatic separator. Continuous white areas are background.

ured for the carbon concentrates is below the value of 0.400 to 0.600 g/cm^3 typical for activated carbons. The lower amount of mass per unit volume of the carbon concentrates is probably due to an abundance of large voluminous pores. The pore distributions shown in Table 2 indicate that the majority of the pore volume in the carbon concentrates can be attributed to macropores. The mesoporosity is very low and microporosity is practically nonexistent.

As noted earlier and reported in Table 3, the calculation of microporosity yielded negative values for half the samples. This is not surprising considering the values were calculated by difference and the independent method of determining porosity by measuring the carbon tetrachloride activities indicated that overall porosity was very small. It has been noted that porosity calculations using envelope and skeletal densities become less accurate when the sample porosity is low.[29] To corroborate the micropore volume values, the t-method for determining microporosity was employed using the limited range of data from the multi-point BET measurements.[30] That method also yielded near-zero micropore volumes. The important conclusion is that all of these measurements indicate that there is very little if any microporosity in these samples. An earlier study also reported extremely small micropore volumes for three unactivated fly ash carbon samples.[31]

A lack of microporosity can severely affect the adsorption properties of carbon particles, as demonstrated by the low iodine numbers and carbon tetrachloride activities measured for the carbon concentrates. Activated carbons typically have iodine numbers in the range of 900 to 1,200 mg/g and carbon tetrachloride activities of 40 to 80%. While nitrogen BET and mercury porosimetry, respectively, provide direct measurements of surface area and porosity, iodine number and carbon tetrachloride activities allow a more direct comparison with parameters measured for activated carbons and serve to independently verify the results of the other tests. Low surface areas and iodine numbers are characteristic of some carbon blacks, which are used more often as fillers than adsorbents. Studies have shown that carbon concentrates from fly ash, despite their poor surface area and low microporosity, can be used for the adsorption of macro-molecules.[17] The adsorption properties of the carbon concentrates also can be enhanced by activation treatments.[9,12,16] Only then can they be used in place of activated carbon.

All of the carbon concentration methods used in this study yielded carbons with most of their pore volume attributable to larger pores, but some methods were more efficient at doing that than others. The PMET concentrates and the MTU2 concentrate had significantly larger macropore volumes and average pore diameters than carbons produced by the other concentration techniques. In the case of the PMET samples, the higher average pore diameter can most likely be attributed to sizing of the sample prior to separation of the carbon. The sizing, or sieving, preselects the larger carbon particles for further concentration. The larger particles are more likely to contain bigger pores. The MTU2 sample was not sized prior to flotation and therefore its particle size was not significantly different from that of the other carbon concentrates. It is more likely that combustion conditions were such that they favored the production of larger pores.

The particle size distributions of the carbon concentrates were very similar, except for the larger size of the PMET sample and the smaller overall size of the NEP1 sample. It is informative to closely examine the change in particle size distributions for the UK1 series in order to determine the effects of processing on particle size. The data in Table 3 show that a single run through a cylindrical dry separator results in an increase in particle size of the carbon concentrate. Much like sieving, it appears that the cylindrical dry separator preferentially selects the larger particles, which are typically carbon-rich.[32,33] In contrast, a single run through a parallel plate triboelectrostatic separator results in a somewhat overall smaller particle size compared to the starting material. In addition, the product of the parallel plate separator is richer in carbon than the product of the cylindrical dry separator. An increase in carbon content accompanied by a decrease in particle size in the parallel plate separator may result from the break up of carbon-ash agglomerates, thereby facilitating the liberation of carbon from the ash. Ash may less likely be liberated from the larger carbon particles when using the cylindrical dry separator, making it more difficult to obtain a purer carbon concentrate. The NEP1 sample has the smallest overall size probably owing to an abundance of finer ash particles in this unprocessed ash.

When the product of a single pass through a parallel plate separator is processed again, an additional slight enrichment in carbon content is observed. While the

(28) Kulaots, I.; Gao, Y.-M.; Hurt, R. H.; Suuberg, E. M. *Proceedings of the 1999 Conference on Unburned Carbon on Utility Fly Ash*; U.S. DOE Federal Energy Technology Center: Pittsburgh, 1999; pp 43−45.

(29) Webb, P. A.; Orr, C. *Analytical Methods in Fine Particle Technology*; Micromeritics Instrument Company: Norcross, GA, 1997; p 210.

(30) Lippens, B. C.; de Boer, J. H. *J. Catal.* **1965**, *4*, 319.

(31) Maroto-Valer, M. M.; Andresen, J. M.; Andresen, C. A.; Morrison, J. L.; Schobert, H. H. *Prepr. Pap.—Am. Chem. Soc., Div. Fuel Chem.* **2000**, *45*, 509−513.

(32) Shibaokg, M. *Fuel* **1986**, *65*, 449−450.

(33) Paya, J.; Monzo, J.; Borrachero, M. V.; Perris, E.; Amahjour, F. *Cem. Concr. Res.* **1998**, *28*, 675−686.

geometric mean sizes reported in Table 3 for samples UK1C and UK1D are not significantly different, the particle size distribution curves that accompanied the results showed that some of the smallest particles in sample UK1C had been further reduced in size upon reprocessing. Therefore repetitive processing of the sample can lead to some additional liberation of carbon from the ash.

Optical microscopic images of the UK1 carbon enriched fly ash sample in Figures 5 and 6, taken at the same magnification, clearly show the effects of multiple triboelectrostatic processing steps on particle size and the liberation of carbon from ash. The primary particle shapes are irregular for the char particles and the ash particles appear as cenospheres. After undergoing triboelectrostatic separation, there are still some larger irregular char particles, but they are now void of much of the ash. Most of the particles have been reduced in size and consist primarily of char fragments with some smaller ash cenospheres. This visual observation is corroberated by the particle size data in Table 3.

Comparison of the incremental intrusion curves in Figure 1 provides additional insight into some similarities of the carbon concentrates. As described earlier, the curves show that the pore volumes of the samples are concentrated in macropores. Also in Figure 1, the distribution of pores is very similar for certain groups of samples. The PMET samples stand out again because of their near normal pore distribution, which is much larger than those of the other samples. The distribution of pores in the UK1 samples does not change significantly when processed using the parallel plate separator despite the observed change in particle sizes. There is some loss of the largest macropores when the sample is processed using the cylindrical dry separator. The NEP2 sample, which was also triboelectrostatically separated, had a pore distribution similar to the UK1 series. Likewise the MTU1 and UK2 samples, which were processed by flotation, also have similar pore size distributions that were different from those of the triboelectrostatically separated sample. The MTU2 sample was also processed by flotation and its pore size distribution has similar features to those of the other two concentrates processed by flotation, but it also has a significant contribution to the overall distribution from its largest pores. Although further investigation is required, the results suggest that the processing methods may be selective for certain pore sizes. Pore size selectivity will be a consequence of particle size selectivity if the carbon is not evenly distributed across the size spectrum.

The similarity in properties of a majority of the carbon concentrates is again shown in the CAPTO and TGA profiles. The CAPTO and TGA profiles for a given sample are nearly identical. The corresponding TGA profile is somewhat broader and shifted to higher temperature probably because of the faster heating rate used in TGA. It is important to note that there are no extraneous peaks in the TGA spectrum for a given sample compared to the CAPTO profile. Because TGA is measuring the weight change due to oxidation of all species in the sample while CAPTO is only measuring oxidation of carbon, the results show that there are no major components in the concentrates, other than carbon, that are undergoing oxidation. This observation is corroborated by the excellent agreement between loss on ignition (LOI) and percent carbon concentrations measured for each sample in this study; the mean difference in LOI and %C measurements for the samples was 1.7 ± 1.3. LOI values have been used in the past as an indirect measurement of unburned carbon in fly ash. It was found that there was poor agreement between LOI values and percent carbon when significant concentrations of Ca-containing species, which oxidize below 1000 °C, were present.[33,34]

The CAPTO and TGA peak envelopes appear to contain a number of component peaks. An attempt has been made to apply factor analysis to determine the minimum number of peaks that, when added together, could adequately approximate the overall peak envelope. Preliminary work has identified five peaks that make up the envelope centered at about 650 °C. However no logical basis for assigning chemical structures to those peaks could be established. It does appear that the position of the envelope is related to the degree of disorder of the carbon structure and the degree of graphitization.[27] The peak for activated carbon, which would have a very high degree of disorder, appears at 400 °C in the CAPTO analysis. Graphite, which has a very low degree of disorder and naturally is highly graphitized, has a peak around 750 °C. Therefore the CAPTO peak positions are indicative of carbons that have an intermediate amount of disorder and are only partially graphitized. The PMET sample has a CAPTO profile much like that measured for metallurgical coke, which exhibits somewhat greater graphitization than most carbons from fly ash.

The degree of graphitization and carbon disorder can also be measured from the Raman spectra by examining the widths of the G band at 1630 cm^{-1} and the D band at 1360 cm^{-1}.[35,36] An increase in width of these bands is indicative of an increase in disorder of carbon and less graphitization. The relative intensities of the bands can also provide the same information, but care must be taken when comparing intensities to literature values because of variation in relative band intensities with excitation source.[36] Some disorder of the carbon crystallites is apparent from the width of the bands in the spectra in Figure 4. Comparison with the relative bandwidths of other carbon materials shows that the carbon concentrates have degrees of carbon graphitization similar to those found for cokes and carbon blacks and are higher than those measured for typical coals.[34] The XRD results also supported the observations made above about the degree of disorder of carbon in the carbon concentrates.

Note that the three samples (MTU1, UK2, NEP1) having the widest bandwidths in the Raman spectra in Figure 4 also have very similar pore size distributions, as shown in Figure 1. Their pore size distributions are more skewed toward the smaller end of the macropore scale compared to the other samples. Therefore there appears to be a relationship between macropore size of a sample and its degree of graphitization. The only

(34) Brown, R. C.; Dykstra, J. *Fuel* **1995**, *74*, 570−574.
(35) Cuesta, A.; Dhamelincourt, P.; Laureyns, J.; Martinez-Alonso, A.; Tascon, D. *Carbon* **1994**, *32*, 1523−1532.
(36) Mennella, V.; Monaco, G.; Colangeli, L.; Bussoletti, E. *Carbon* **1995**, *33*, 115−121.

exception is for the PMET sample, which would be expected to have a higher degree of graphitization based on its pore volume distribution. A relationship between degree of crystallinity and porosity has implications regarding the reactivity of the carbons because increased graphitization has been associated with loss of porosity and active sites on the carbon surface.[25] Reflectance values can also be correlated to the amount of disorder in the carbon particles.[37] The values in Table 2 agree with the other results that show a similar degree of disorder among the carbon samples; only the MTU2 sample appears to have a relatively higher degree of order.

Additional information about the microstructure of unburned carbon that may impact its utilization can be gained from petrographic analyses. Three forms of unburned carbon char/coke are typically present in fly ash. The char particles consist of anisotropic carbon and isotropic carbon formed from the incomplete combustion of vitrinite macerals. Inertinite can be carried over as unburned carbon because it is not easily altered by combustion. Isotropic carbon particles are highly disordered and porous while anisotropic carbon particles have a more aligned microtexture. The relative amounts of anisotropic and isotropic coke in the fly ash are indicative of the type coal that was burned. Burning of higher rank coals leads to a greater proportion of anisotropic coke in the ash.[38] The relative proportions of isotropic and anistropic particles in unburned carbon from coal-combustion fly ash can vary greatly.[16,39]

The dominant carbon form in all of the concentrates used in this study was anisotropic. This agrees with the observations of thermal analyses, which placed the carbons closer to graphite than highly disordered activated carbon. It also agrees with the porosity measurements, which show the chars to have low porosity and surface areas. Anistropic particles are also expected to have high densities, consistent with the values reported in Table 2.[40] On the basis of the reactivities previously found for the two forms of carbon,[16,21] the highly anisotropic carbon concentrates would be expected to be relatively inert and have poor adsorption capacities. This was borne out in separate tests of the UK1 set of samples for their capacity to absorb mercury from flue gas.[14] The UK1 carbon concentrates had among the lowest adsorption capacities out of all the materials that were tested in that study. Not surprisingly, the adsorption capacity of the UK1 series of carbons did increase with carbon concentration.

Another recent study indicated an apparently higher adsorption capacity for anisotropic coke compared to isotropic coke.[13] This seems to be opposite what would be expected based on the discussion above and in fact the author noted the possible discrepancy with the results of a previous study. One reason for the discrepancy may simply be trying to compare small differences in mercury adsorption and surface area in materials that themselves have small mercury adsorption capacities and surface areas. It has also been shown that factors other than pore volume and surface area may play important roles in determining the adsorption properties of unburned carbon.[23,41]

Summary

The physical properties of the carbon concentrates were similar in many respects despite the variety of sources from which they were obtained and the different types of processing conditions used to produce them. In the case of the PMET samples, sizing of the carbon prior to processing selectively segregates the larger carbon particles, which in turn have some unique physical properties compared to the other carbons. Other processing conditions appear to have a negligible effect on the properties of the carbons except for particle size. Mechanical separation leads to attrition of the particles while flotation separation is expected to have a lesser effect on particle size. Unprocessed ashes typically contain a mixture of small mineral and larger char particles. The particles can be separate or interlocked. Processes that reduce particle size or break up particle agglomerates as part of the separation process should facilitate separation of the minerals from the carbon.

Based on the results presented here, unburned carbon concentrates from fly ash do not hold much promise as replacements for activated carbons in adsorption processes. This does not preclude activating the carbon concentrates in a separate processing step. Additional experiments are being conducted to test the viability of that approach. The poor adsorption properties of the unburned carbon may still be important to the concrete industry, where fly ash is used as a cost-saving additive. Other adsorption mechanisms may play a role in the carbon's interference with the behavior of air-entrainment agents commonly added to concrete mixtures. Because unburned carbon was found to have many of the properties of carbon black, it may have immediate applications for use as fillers and in processes and materials as a substitute for carbon black, provided that the unburned carbon can be processed to sufficient purity.

Acknowledgment. The authors acknowledge J. Stencel and J. Groppo of the University of Kentucky (CAER), C. Koshinski of PMET, J. Hwang of MTU, and M. Rook of New England Power for providing the samples used in this study. H. Nowicki of PACS provided valuable assistance in interpreting some of the results.

(37) Johnson, C. A.; Patrick, J. W.; Thomas, K. M. *Fuel* **1986**, *65*, 1284−1290.

(38) Graham, U. M.; Hower, J. C. *Management of High Sulfur Coal Combustion Residues: Issues and Practices, Conference Proceedings*; National Technical Information Service: Springfield, VA, 1994; pp 80−90.

(39) Hower, J. C.; Trimble, A. S.; Eble, C. F.; Palmer, C. A.; Kolker, A. *Energy Sources* **1999**, *21*, 511−525.

(40) Maroto-Valer, M. M.; Taulbee, D. N.; Hower, J. C. *Energy Fuels* **1999**, *13*, 947−953.

(41) Kulaots, I.; Gao, Y.-M.; Hurt, R. H.; Suuberg, E. M. *Prepr. Pap.—Am. Chem. Soc., Div. Fuel Chem.* **1998**, *43*, 980−984.